



Atomic force microscopy study of the biofouling and mechanical properties of virgin and industrially fouled reverse osmosis membranes

L.C. Powell^a, N. Hilal^b, C.J. Wright^{a,*}

^a Biomaterials, Biofouling and Biofilms Engineering Laboratory (B³EL), The Systems and Process Engineering Centre (SPEC) College of Engineering, Swansea University, Fabian Way, Swansea, UK

^b Centre for Water Advanced Technologies and Environmental Research (CWATER), College of Engineering, Swansea University, Fabian Way, Swansea SA1 8EN, UK

HIGHLIGHTS

- Atomic force microscopy (AFM) imaging of industrially fouled reverse osmosis membranes
- AFM force spectroscopy measured the Young's modulus of virgin and fouled membranes.
- pH influenced the mechanical properties of virgin and fouled membranes.
- AFM force spectroscopy of membranes extended to measure energy of adhesion.
- Significant difference in mechanical properties between fouled and virgin membranes

ARTICLE INFO

Article history:

Received 13 June 2016

Received in revised form 27 October 2016

Accepted 5 November 2016

Available online 23 November 2016

Keywords:

Membrane

Reverse osmosis

Biofouling

Biofilm

Atomic force microscopy

ABSTRACT

The mechanical properties of virgin and industrially fouled reverse osmosis membranes (composite polyamide) used for the purification and desalination of seawater in desalination processes were characterised using novel atomic force microscopy (AFM) methods. Polymeric surface elasticity has previously been demonstrated to strongly affect the adhesion of bacteria; hence the study examined membrane surface elasticity to demonstrate how AFM can be used to assess the bio-fouling potential of membranes. An AFM colloid probe technique was used to determine the mechanical properties of the membrane, the adhesion forces and the work of adhesion at the membrane surfaces. The mean values of Young's modulus for the virgin membrane decreased in magnitude with increasing pH values, where these values were significantly different ($p < 0.017$) between both pH 3 (1450 kPa), pH 7 (1327 kPa) and pH 9 (788 kPa). These differences were attributed to differences in membrane swelling and indicate possible control parameters that could be exploited to improve membrane cleaning regimes. A membrane with a higher modulus will be stronger and potentially more resistant to chemical and physical processes during operation and cleaning. Significant differences ($p < 0.017$) in force measurements were also found between different electrolytic conditions for each of the membranes, where for the virgin membrane the adhesion force values were 6.00 nN at pH 3, 1.77 nN at pH 7 and 0.98 N at pH 9, and also the work of adhesion were 153.6 nJ at pH 3, 22.8 nJ at pH 7 and 9.9 nJ at pH 9 in 0.6 M NaCl. These observations further confirm the importance of the electrolytic environment on the nanoscale interactions of the membrane which should be considered to control fouling during operation and cleaning cycles. AFM images and streaming potential measurements of virgin and fouled membranes were also obtained to aid analysis of the industrial membrane system. The novel application of AFM to membranes to measure Young's moduli and work of adhesion is a new addition to the AFM tools that can be used to unravel separation processes at the membrane surface. In addition, this study further demonstrates that AFM force spectroscopy can be used as part of a sophisticated membrane autopsy procedure for the elucidation of the mechanisms involved in membrane fouling.

© 2016 Elsevier B.V. All rights reserved.

1. Introduction

Membrane separation is now an established technology that has been applied for the production of ultra-pure water by the purification

and desalination of seawater using reverse osmosis (RO) membranes. However, membrane filtration processes are commonly impeded by membrane fouling, which leads to considerable technical problems, such as reduction in water product quality and requirement for higher pressure. The life span of the membrane is also shortened by fouling and the subsequent need for cleaning processes [1,2]. A major contributing factor to membrane fouling within industry is the formation of

* Corresponding author.

E-mail address: c.wright@swansea.ac.uk (C.J. Wright).

microbial biofilms at the surface of the membrane [3,4]. Desalination plants can use a number of strategies for the prevention and control of membrane fouling, which include the use of pre-treatment units for the removal of organic and inorganic dissolved substances and the cleaning of the membrane by either back-washing or chemical wash [5]. To augment these strategies many studies have focussed on the membrane fabrication stage to reduce fouling and optimise the membrane processes [6,7]. Thus, a greater understanding of the physical, chemical and biological processes regulating biofilm formation and development is required to aid in developing new strategies to inhibit or control the biofilm membrane fouling.

Atomic force microscopy (AFM) has become an essential tool for the membrane technologist optimising separation processes through greater understanding of fouling mechanisms [8–10]. This versatile instrument not only produces high resolution images of the membrane surface in process relevant environments but can also be used to quantify the forces acting at a membrane surface which govern fouling processes. Force is measured as a function of distance when a probe attached to the apex of the AFM cantilever, approaches the sample, makes contact and then retracts away from the sample. The displacement is varied using the extension and retraction of a piezoelectric crystal. The deflection of the cantilever is monitored and converted into values of force using Hooke's Law, calibration of the spring constant and deflection sensitivity [11]. Force measurement data presented in the form of a force-distance curve, as shown in Fig. 1, can provide valuable information on interactions forces and local material properties such as elasticity, hardness, adhesion and surface charge densities. Fig. 1 presents typical AFM measurements made at virgin and fouled membranes within an aqueous environment. The local mechanical properties of a membrane or fouling layer indicate the resilience of the material to chemical and physical processes. For polymer membranes a harder surface may have reduced wear compared to softer membranes during operation and cleaning cycles [12]. A foulant layer which has low mechanical robustness will be more susceptible to hydrodynamic shear applied during cleaning procedures. The mechanical properties of a membrane or a thin film can be studied by measuring force-distance curves obtained by AFM and then analysing force data through a chosen mechanical theory which considers the contact and indentation of two surfaces to obtain a value of Young's modulus. AFM imaging can be used to identify changes in nanoscale morphology and surface roughness when a foulant layer forms on a membrane surfaces. AFM force-distance curves can be used to measure changes in the mechanical properties at the membrane surface when the membrane-fouling layer system forms.

AFM imaging has been used to study the surface roughness and pore size distribution of many types of membrane, the distribution of fouling materials at a membrane surface before and after cleaning processes [13,14] and also to study the early bacterial colonisation events that lead to biofilm formation at nanofiltration membranes [15]. The AFM force-measurement capability has been used to study interactions that govern separation processes including particle/bubble interactions [16] and particle/membrane interactions to provide an assessment of the fouling potential of membranes [17,18]. The bulk mechanical properties of membranes, such as polybenzimidazole (PBI), have been investigated for the determination of tensile strength, storage modulus and Young's modulus, using techniques such as dynamic mechanical analysis (DMA) [19,20]. However, the local mechanical properties of the polymer, at the membrane surface, vary from the bulk of the polymer, and it is the local properties that act at the commensurate size of microbes which will influence the microbial attachment. The AFM nano-indentation technique allows for a simple, convenient measurement of local Young's modulus of membranes. Franceschini and Corti [21] determined the elastic moduli of nafion, PBI and poly [2,5-benzimidazole] membranes, both undoped and phosphoric acid doped, using AFM force spectroscopy. AFM nano-indentation has also been used to measure the Young's modulus and hardness of various polymers, such as polyethylene, polyvinyl alcohol, polyvinyl chloride, polycarbonate,

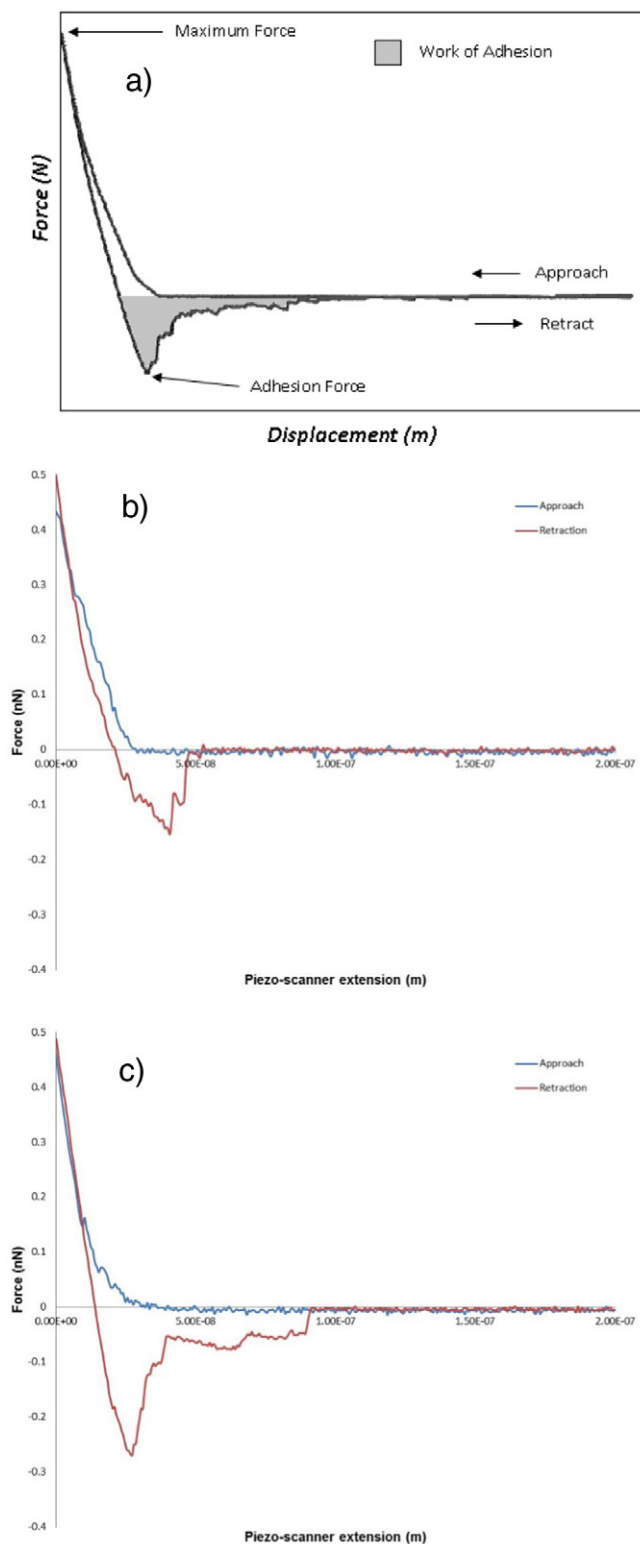


Fig. 1. Force-distance measurement curves: (a) Annotated AFM force curve typically measured over 1 μm , (b) typical AFM force curve measured within liquid at a virgin membrane and (c) typical AFM force curve measured within liquid at a fouled membrane.

Nylon6, poly(methyl methacrylate), polystyrene and polyacrylic acid [22,23]. However, there is a limited literature on the membrane elasticity of commercially available membranes, and it is only recently that Chung et al. [24] reported the first measurement of the Young's modulus of the active layer of RO membrane using a combined wrinkling-cracking methodology.

Many studies that have used AFM to characterise virgin and fouled membrane surfaces have only measured adhesive forces and have been limited as they have used small numbers of AFM force-distance measurements to characterise the surfaces. Recent developments in AFM technology and its associated data capture now permit the measurement of multiple force measurements across a surface and the creation of force measurement distributions. This has enabled statistical analysis and improved comparison between different surface systems including fouled membranes [13,25].

AFM has been used extensively for the study of bacteria but only a few researchers have used this technique to study biofilms [26,27]. AFM imaging has provided high resolution images of the bacterial cell surface and AFM force measurement has been used to quantify bacterial cell-surface adhesion. The AFM nanoindentation technique allows the measurement of substrate elasticity and is being used to unravel the fundamental processes involved in the attachment of cells and bacteria to elastic surfaces. Recently substrate elasticity has emerged as an important physical factor in the response of many cell types to surfaces. Some research groups consider that the elasticity of a substrate will have an effect on the cell rigidity; therefore the stiffness of a substrate is intrinsic to the cells response of attachment and growth [28–30]. A few studies were performed on the mechanical properties of bacterial cells grown on soft elastic surfaces. Bakker et al. [28] investigated the deposition of three marine strains, *Halomonas pacifica*, *Marinobacter hydrocarbonoclasticus* and *Psychrobacter* sp. onto polyurethane coated glass with varying elastic modulus in a stagnation point flow chamber. It was shown that the bacteria adhered in higher numbers to hard surfaces compared to that at surface coatings of lower elastic moduli. Lichter et al. [30], engineered weak polyelectrolyte multilayered (PEM) thin films within the elasticity range $1 \text{ MPa} < E < 100 \text{ MPa}$ to investigate if surface elasticity affects bacterial adhesion. The adhesion of viable *Staphylococcus epidermidis* and *Escherichia coli* was found to correlate positively with increasing elastic modulus of PEM, independently of surface roughness, surface interaction energy and surface charge density of the surface. These studies demonstrate that the stiffness of nanoscale polymeric substrata can strongly affect the adhesion of bacteria from aqueous suspensions and that the measurement of local mechanical properties of a substrate and bacterial cells are required for the understanding of cell responses on surfaces [29]. Oh et al. [31] have also observed that the formation of a bio-fouling layer (biofilm) is strongly dependent on the mechanical characteristics of the solid substrate. Therefore, membrane elasticity is a key factor in bacterial cell attachment and hence biofilm formation, where force measurements could provide an assessment of membrane bio-fouling potential within process environments. Therefore, in the present study a comprehensive AFM force measurement investigation was performed on both virgin and industrially fouled commercial RO membrane surfaces; the membrane samples were removed from a desalination plant, for pre-treated seawater, that was experiencing fouling. This was to determine the micromechanical properties of the systems as indicators of their propensity for biofouling and also for the development of fouling control regimes for optimisation of membrane processes and water treatment. This was achieved through obtaining Young's modulus values, adhesion force and work of adhesion at different pH values and in media containing the salt content of seawater. Surface charge measurements were also performed on the membranes surfaces to further examine the processes of adhesion. It is the first time, to the author's knowledge, that AFM nanoindentation experiments have been performed on RO membranes and on industrially fouled membranes for the measurement of elasticity properties.

2. Materials and methods

2.1. Membrane preparation

The membrane element, SWC3 +, used was obtained from Hydranautics (Nitro Denko Company). The membrane polymer is composite

polyamide and has a nominal salt rejection of 99.8%. An industrially fouled section of the membrane element, SWC3 +, was obtained from the Fujairah Water and Power plant, located in the United Arab Emirates (UAE). The fouling was known to be bacterial in origin; a culture independent method based on the 16S rDNA sequence and constructed gene libraries for the identification of the microbial diversity was used to identify the most significant bacteria responsible for biofilm formation and biofouling at the industrial RO membrane system of the present study [3]. *Proteobacteria* was determined to be the most abundant identified group, with γ -*Proteobacteria* being the most predominant class within the phylum. The next most abundant grouping was the *Bacteroidetes* and *Planctomycetes*. The fouled membrane section was stored at -20°C until used. Storage may impact on the structure of the foulant layer, this is a problem that is innate to all such studies which remove bio-fouled samples from a process environment to facilitate membrane study. However, in this case the thin foulant film may be protected by the underlying substrate membrane. Prior to AFM analysis, the virgin and industrially fouled membrane samples were soaked in deionised water at 4°C for 24 h, taking care not to disrupt the foulant layer present on the industrially fouled membrane. In preparation for imaging after 24 h of initial soaking, the virgin and industrially fouled membrane samples were left to dry then cut into small sections of 15 mm^2 within a sterile environment and attached to one side of a glass cover slip using double sided adhesive tape.

In preparation for AFM force measurements, the virgin and industrially fouled membrane samples were cut into small sections within a sterile environment and attached to one side of a 25 mm^2 circular glass cover slip using double sided adhesive tape. A circular 25 mm^2 plastic fluid cell was then placed over the cover slip and secured in place with silica gel. 3 ml of the liquid of varying pH and salt concentration was placed carefully into the fluid cell and left for 20 min for the system to stabilise.

In preparation for streaming potential measurements, the virgin and industrially fouled membrane samples were cut using provided templates (Anton Paar) into two rectangular shaped pieces with specific holes for liquid flow, which would fit the rectangular fluid cell of the instrument.

2.2. Membrane AFM images

A Dimension 3100 AFM (Bruker) was used for membrane imaging. Noncontact cantilevers were used for imaging (OTESPA, Bruker). The membrane images were achieved using tapping mode within an air environment of 21°C and a relative humidity of 40%. Tapping mode AFM has been used extensively to image membranes and microbial surfaces [8,9,11]. Tapping mode in air was used and not imaging in liquid, the latter is experimentally demanding and risks imaging artefacts by damaging diffuse foulant layers if present. A scan rate of 0.4 Hz was used for most images, however for the largest scan size of $100 \mu\text{m} \times 100 \mu\text{m}$, a scan rate of 0.2 Hz was used to achieve a higher quality image. The images were analysed through the AFM Nanoscope software to obtain peak to valley and surface roughness measurements for both the virgin and fouled membranes at each scan size.

2.3. Force spectrometry measurement of local elastic properties

The NanoWizard II BioAFM with top view optics (JPK Instruments) was used for the force measurements on all membrane surfaces. AFM colloid probes were made using a micromanipulator (Singer Instruments). In this technique a silica sphere of $3 \mu\text{m}$ radius was attached to the apex of a tipless cantilever using glass bond glue. Only AFM colloid probes of radius $3 \mu\text{m}$ were used in experimentation to standardise the contact area between the probe and the surface. The colloid probe's cantilever spring constant was measured via the thermal tune method. The silica colloid probe was chosen for indentation studies of the membranes due to its well defined shape and larger tip radius when

compared to manufactured silicon nitride sharp tips [32]. This means that on a soft surface, the silica colloid probe will more likely compress the surface, unlike sharp tips which could puncture and disrupt the surface as sharp tips induce local strains that can far exceed the linear material regime. 50 force curves were measured across the membrane surfaces at randomly chosen locations in each experimental system.

2.4. Streaming potential of the membranes

The Electro Kinetic Analyzer (Anton Paar) was used to determine the streaming potential of virgin and industrial fouled membranes at 0.1 M NaCl concentration and pH values 3–9. The cut membrane sample pieces were clamped between two measuring cell parts separated by a defined streaming channel within the rectangular fluid cell. Once the preliminary rinse cycles were performed, the pH of the salt solution was adjusted and the zeta potential measurements were repeated three times for each pH value in each direction of fluid flow. Zeta potential of the membrane surfaces was calculated from the measured streaming potential using the Helmholtz-Smoluchowski equation with the Fairbrother-Mastin approach.

3. Data analysis

The AFM force data was analysed to determine values of maximum adhesion force, work of adhesion and the Hertz model was used to calculate Young's Modulus values. The value of force is calculated from the deflection of the cantilever using Hooke's law. The force as a function of the piezo scanner displacement is sufficient to calculate the parameters and no further manipulation of the piezo scanner displacement data is required. The contact region of the approach curve is compared to that measured at a hard un-deformable surface to calculate the indentation depth (h) when a force (F) was applied [27]. The value of adhesion is determined from the minimum point of the retraction curve. The contact point was defined as the height where the cantilever deflection begins to leave the horizontal axis on the deflection vs. sample height curve [33]. The work of adhesion was determined from the area between the retraction curve and the x axis (Fig. 1) applying the trapezoidal rule to integrate.

The equation widely used to calculate the force on the cantilever $F(h)$ by using Hertz mechanisms is [11]:

$$F(h) = \frac{4\sqrt{R}}{3} E^* h^{3/2}$$

The tip is approximated by a sphere with the radius R . E^* is known as the effective modulus of a system tip-sample. The material of the tip is considerably harder than the sample, thus the following equation was used:

$$E^* \approx \frac{E_{\text{sample}}}{1 - \nu_{\text{sample}}^2}$$

where E_{sample} and ν_{sample} are the denotations for the Young's Modulus and the Poisson ratio for the materials of the sample, respectively. Through the substitution of the above equations into the Hertz equation and analysis of the data from the force-distance curves, the Young's Modulus of the sample was determined.

3.1. Statistical analysis

All data are expressed as mean \pm standard deviation. The statistical analysis was performed using MiniTab Software, where normal distribution of variables was assessed using the Krustill Wallis test. The non-parametric Mann-Whitney U test for independent samples was used to compare mean values of adhesion force, work of adhesion and

Young's modulus between virgin and fouled membranes. Due to multiple testing, a Bonferroni correction was applied for each analysis.

4. Results and discussion

4.1. High resolution images

Atomic force microscopy imaging elucidated the morphology of the fouling layers at the industrial fouled RO membranes. Fig. 2 presents high resolution $10 \times 10 \mu\text{m}$ and $100 \times 100 \mu\text{m}$ AFM topographical images of virgin and process fouled SWC 3 + RO membranes. The virgin membrane images clearly show the structure of the RO membrane surface, where the structural surface of the membrane is composed from peaks and valleys. A similar RO surface topography was observed in an AFM and SEM study by Kwak and Ihm [34]. The fouled membrane images clearly show the relatively non-uniform distribution of fouling present on the RO surface, where the structure of the RO membrane can be seen in gaps within the fouling layer (Fig. 2B). The high resolution images of the fouled membranes suggested the presence of a bacterial biofilm, with the presence of particles of commensurate size of bacteria embedded in a loose film like structure. The presence of the bacterial biofilm was further supported by previous work that used standard DNA techniques to identify the key bacterial species involved in the industrial fouling of the membrane of this study [3]. AFM technology has previously been utilized for the low resolution imaging of foulant layers formed on process membranes [35,36].

The surface roughness and peak to valley measurements are shown in Table 1, where the root mean square (RMS) surface roughness of the virgin RO membrane was $174 \pm 26 \text{ nm}$ and the peak to valley measurement of $1975 \pm 757 \text{ nm}$ and the RMS surface roughness of the fouled membrane was $297 \pm 44 \text{ nm}$ and peak to valley measurement of $3837 \pm 1013 \text{ nm}$ measured from the $100 \times 100 \mu\text{m}$ images. The results also show that as the scan size increases from 1 to $100 \mu\text{m}^2$, the values of surface roughness and peak to valley increase for both the virgin and fouled membranes. The current results agree with the work of Boussu et al. [37] which found that surface roughness increases with scan area from $0.5 \mu\text{m}^2$ to $10 \mu\text{m}^2$ with different NF membranes, where an explanation is that when the scan size is changed, it is possible to get a different surface topography, therefore resulting in a different roughness value [37]. From Table 1, it can also be seen that the fouled membrane surface has the largest surface roughness and peak to valley measurements for all scan sizes when compared to the virgin membrane, apart from the surface roughness values measured from the $10 \times 10 \mu\text{m}$ image, where the fouled membrane surface is smoother than the virgin membrane. The smoother surface could be due to the presence of a cohesive fouling layer, which may have been facilitated by bacterial fouling producing extracellular polymeric substance (EPS) within the foulant layer. Previous research has found that surface roughness measurements of similar, virgin RO membranes were 66 nm [38] (from $4 \times 4 \mu\text{m}$) and 50 nm [34] (from $10 \times 10 \mu\text{m}$) and the corresponding peak to valley measurements were 560 nm [38] and 400 nm [34]. The range of these values confirm with current findings of surface roughness and peak-to-valley measurements of virgin RO membranes at small scan sizes (Table 1). The topography, surface roughness and peak to valley measurements show that the virgin RO membranes could be susceptible to biofouling, as the rough surface topography, with valleys of size commensurate with that of bacteria, could facilitate attachment of bacterial cells and shield the attached bacteria from the shear flow.

4.2. Young's modulus measurement by force spectrometry analysis

The mean Young's modulus values were determined from force measurements achieved at virgin and fouled membranes in 0.6 M NaCl at pH values of 3, 7 and 9 (Table 2). The distribution of Young's modulus values from the virgin membrane and fouled membranes are summarized using boxplots shown in Fig. 3, where the distribution of

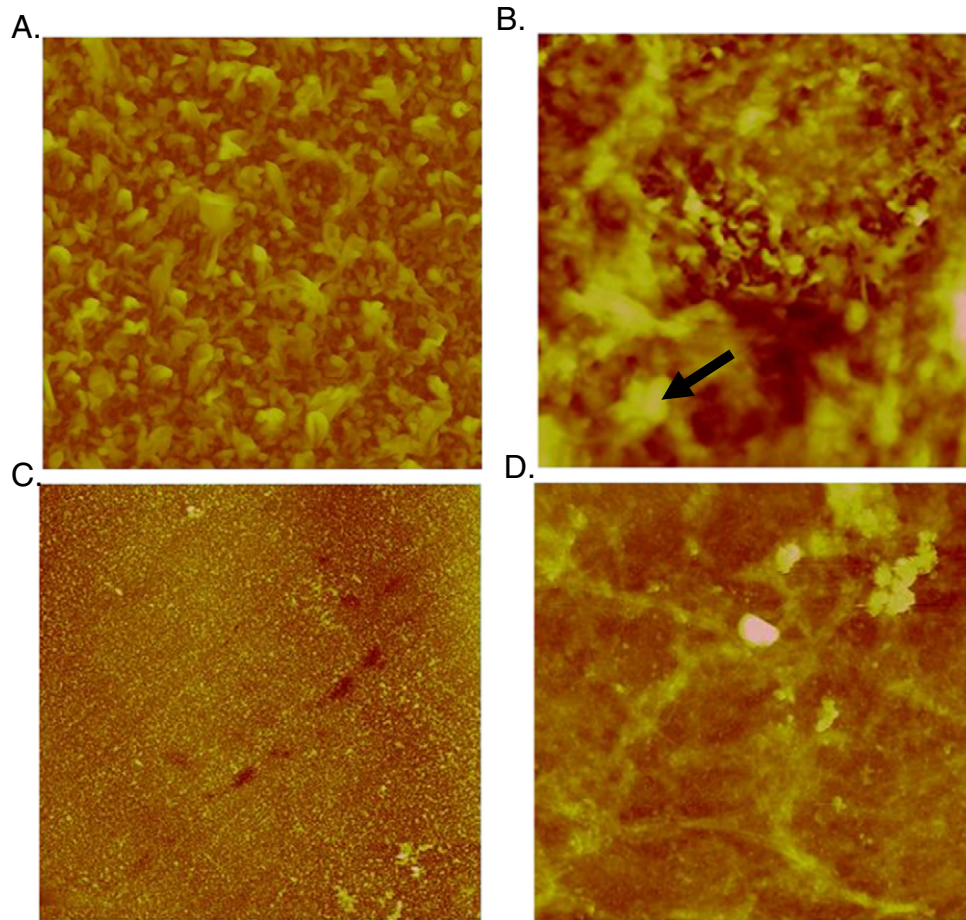


Fig. 2. Tapping mode AFM topographic images of virgin and fouled SWC 3 + RO membrane. A and C images show the topography of virgin SWC 3 + membrane at $10\ \mu\text{m} \times 10\ \mu\text{m}$ and $100\ \mu\text{m} \times 100\ \mu\text{m}$, respectively, while B and D images show the topography of fouled SWC 3 + membrane at $10\ \mu\text{m} \times 10\ \mu\text{m}$ and $100\ \mu\text{m} \times 100\ \mu\text{m}$ respectively. The arrow in image B is suggested to be a cluster of bacterial cells. Z range in all images is $2.0\ \mu\text{m}$.

all variables were non-parametric. The mean values of Young's modulus for the virgin membrane decreased in magnitude with increasing pH values, where these values were significantly different ($p < 0.017$) between pH 3 (1.45 MPa) and pH 9 (0.79 MPa) and pH 7 (1.33 MPa) and pH 9. The change in Young's modulus values with pH could be due to polymer expansion. Elliott et al. [39] has shown that expansion of the ionic polymer film was related to the solution pH. Yang et al. [40] also demonstrated that the ionization of functional groups through pH change plays a key role in the expansion of the membrane, where for certain membranes the higher the pH above the IEP in terms of zeta potential can lead to favourable polar interactions with the surrounding solution so that the foulant compounds are more extended. The IEP of the polyamide membrane in this study is at low pH (Section 4.5). Thus, the higher Young's Modulus at lower pH coincides with a membrane that has a denser polymeric structure. These results indicate that the electrolytic environment is a potential control parameter that could be exploited to improve the mechanical robustness of a polymer membrane, where at pH 3 the surface is at its most robust with the highest Young's modulus measured for all electrolytic environments

tested (1.45 MPa). These results could provide the membrane technologist with a method to improve the maintenance of membrane structure during the chemical and physical challenges of operation and cleaning.

The mean values of Young's modulus for the fouled membrane increased from pH 3 to pH 7 and then decreased in magnitude from pH 7 to pH 9, where these values were only significantly different ($p < 0.017$) from pH 7 (93.8 kPa) to pH 9 (48.0 kPa). The mechanical properties of the fouling layer present on RO membrane surface will affect the shape and stability of the layer and therefore can determine the failure and detachment of the fouling layer in reaction to a physical force such as fluid-induced shear and also the accumulation of such fouling layers in industrial environments [41]. The dependence of the membrane foulant layer Young's modulus on pH could be due to the nature of the different foulant materials within the biofilm and their difference response to the environmental conditions. Therefore the elasticity of the foulant surface present on the membrane surface could vary with industrial conditions. This suggests that optimum electrolytic conditions could be determined where the elasticity of the foulant layer is at its

Table 1
Surface roughness measurements from the virgin and process fouled membrane.

Membrane size (μm)	RMS (nm)		Peak to valley (nm)	
	Virgin	Process fouled	Virgin	Process fouled
1×1	69.7 ± 13.7	87.5 ± 11.2	444.3 ± 112.1	490.2 ± 109.6
10×10	107.9 ± 9.68	99.6 ± 14.3	786.0 ± 116.6	824.3 ± 112.5
100×100	173.7 ± 25.9	297.7 ± 44.2	1974.7 ± 756.8	3837.0 ± 1013.3

Table 2

Mean values of Young's modulus, adhesion force and work of adhesion achieved from both virgin and fouled membranes at various pH values.

	Mean Young's modulus (kPa)		Mean adhesion force (nN)		Mean work of adhesion (nJ)	
	Virgin	Fouled	Virgin	Fouled	Virgin	Fouled
pH 3	1450 ± 986	70.9 ± 36.3	6.00 ± 4.02	0.73 ± 0.90	153.6 ± 89.8	16.2 ± 48.4
pH 7	1327 ± 947	93.8 ± 55.1	1.77 ± 1.14	0.85 ± 0.96	22.8 ± 28.6	13.4 ± 23.9
pH 9	788 ± 432	48.1 ± 26.4	0.98 ± 0.72	0.84 ± 0.85	9.9 ± 10.2	12.9 ± 21.9

lowest, rendering cleaning regimes, such as cross-flow, more effective in removing and breaking up the foulant biofilm.

The comparison between the values of Young's modulus achieved from the virgin and fouled membrane at each pH value showed that all the values of Young's modulus of the virgin were significantly different from the Young's modulus of the fouled membrane ($p < 0.017$), where the values of Young's modulus were greater in magnitude for the virgin membrane (1450 kPa at pH 3) than that for the fouled membrane (70.9 kPa at pH 3). The measurement of Young's modulus can be used to compare the fouling within different process conditions for optimisation, in that lowering the mechanical robustness of the fouling layer and/or raising that of the membrane surface will enable the cleaning regime to be more effective.

Franceschini and Corti [21] performed AFM force measurements to determine the elastic moduli of nonhydrated nafion, PBI and poly [2,5-benzimidazole] membranes, using a sharp contact tip in a N_2 environment, where the elasticity values measured for the different membranes ranged from 0.104 ± 0.036 to 6.17 ± 0.93 GPa. Chung et al. [24] reported the first measure of Young's modulus of the active layer of RO membrane, both in a dry (1.40 ± 0.53 GPa) and hydrated state (0.36 ± 0.14 GPa), using a combined wrinkling-cracking methodology. The difference between these values and those measured in this study are due to the environment in which the measurements were taken and the level of membrane hydration. The indentation experiments in the present study are performed in a liquid environment, as would be in the industrial process, and a colloid probe was used which could also account for this difference in elasticity values; measurements made using a sharp AFM tip will be based on material rupture during layer penetration rather than compression by the colloid sphere. In addition, the studies performed here are industrially relevant with ionic concentrations which would be present within the desalination process, unlike other studies.

4.3. Adhesion force

The mean adhesion force values were determined from force measurements achieved at virgin and fouled membranes in 0.6 M NaCl at pH 3, 7 and 9, where the data is shown in Table 2. NaCl was chosen for the electrolytic media to keep the experimental environment simple,

however the lack of divalent and trivalent ions, which can influence colloidal interaction, may limit extension of the results to seawater. The distribution of adhesion force values from virgin and fouled membranes are summarized using boxplots shown in Fig. 4, where the distribution of all variables were non-parametric. The mean values of adhesion force for the virgin membrane revealed a high adhesion force of 6.0 nN at pH 3, where the values of adhesion force decreased with increasing pH, as measurements of 1.8 nN at pH 7 and 1.0 nN at pH 9 were obtained. The mean adhesion force values were significantly different ($p < 0.017$) between all pH values. The differences in adhesion force values could be due to the charge held by the membrane surface in various electrolytic environments (see Section 4.5). The material that will foul a reverse osmosis membrane will be highly heterogeneous containing materials that are biological in origin including humic acids (a naturally occurring breakdown product of organic matter) and biofilm materials such as xanthan, hyaluronan and dextran. Thus, there will be a range of interactions occurring between fouling material, membrane and the silica probe, including electrostatic, van der Waals and hydrophobic. The amount of information that can be inferred from the measurement of adhesion of an inorganic silica particle at a membrane surface is limited as reverse osmosis membrane fouling is a multi-component process, however the interaction of the colloid probe can be used as an indicator of the degree of particle interaction with that surface. This will be more relevant to the surface interaction with inorganic particles rather than biological particles where specific macromolecular interactions may dominate. It should be noted that many bacteria have a negative charge similar to that of a silica colloid. Thus, the significant differences ($p < 0.017$) in adhesion at the virgin membrane surface as the pH is changed demonstrates that some fouling could be reduced at this membrane surface by controlling the pH. However, this should be considered with reference to pH tolerance of the membrane material and how the electrolytic environment affects the mechanical properties of the membrane (as discussed in Section 4.2) as previous research has observed the bacteria adhere to harder surfaces [28].

The average values of adhesion force for the fouled membrane showed very little variation between the different pH values, where the adhesion force value at pH 3 was 0.7 nN. The mean values were not significantly different ($p > 0.017$) between all pH values, so it was concluded that pH did not have a measurable influence on the values

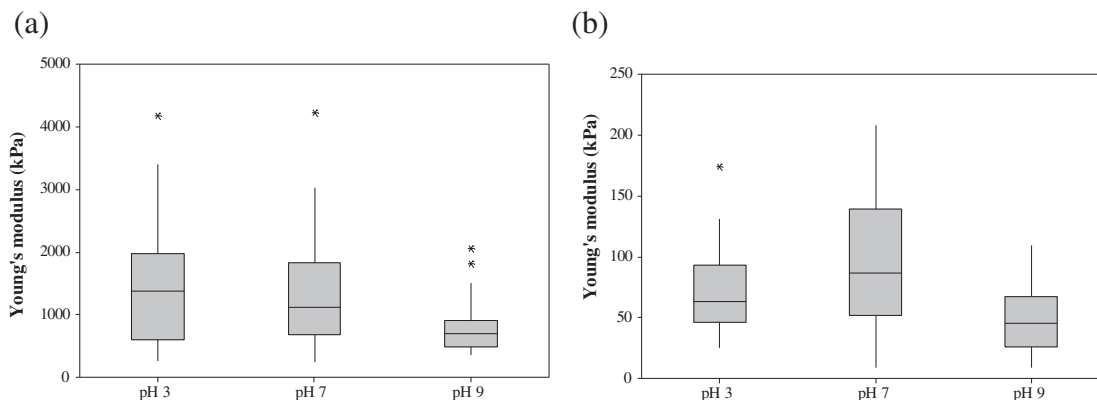


Fig. 3. Variation of Young's modulus of (a) virgin and (b) fouled membranes between different pH values shown in boxplot forms.

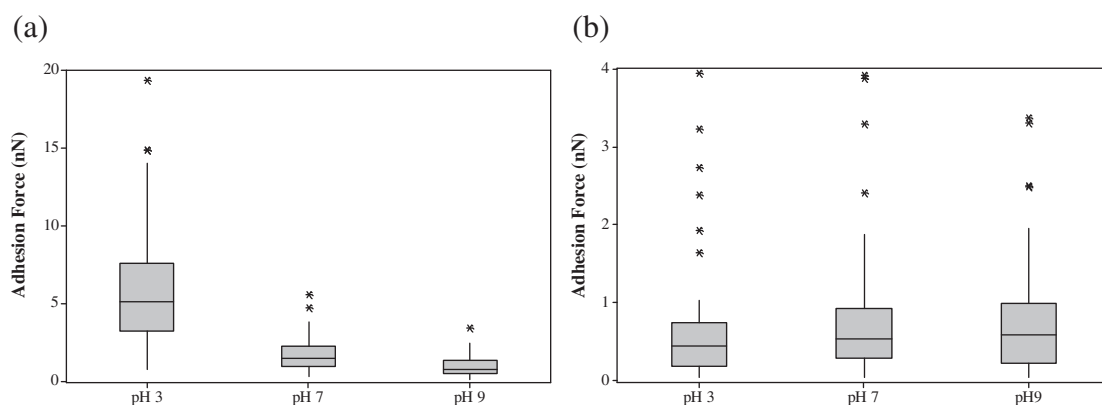


Fig. 4. Variation of adhesion force of (a) virgin and (b) fouled membranes between different pH values shown in boxplot forms.

of adhesion force. This was expected, the chemical heterogeneity of the fouling material will mean that different chemical groups will be ionised to different degrees within the different pH environments, thus there will be no net change in the interactivity of the fouling film. The extent of electrostatic interactions will be reduced within the high ionic strength environment of the present research, thus another explanation for the consistency of adhesive force measured at the different pHs could be the dominance of hydrophobicity on the interaction of the colloid probe and the fouled surface.

The comparison between the values of adhesion force achieved from the virgin and fouled membrane at each pH value revealed that the values of adhesion force of the virgin membrane at pH 3 (6.0 nN) and pH 7 (1.8 nN) were significantly different from the adhesion measured at the fouled membrane at pH 3 (0.7 nN) and 7 (0.9 nN) ($p < 0.017$), apart from the adhesion force values at pH 9 which were not significantly different ($p > 0.017$). The values of adhesion force achieved from the virgin membrane at pH values of 3 and 7 were greater in magnitude than that obtained for the fouled membrane. The differences in adhesion forces observed between the fouled and virgin membrane indicate that the surfaces are chemically different and confirm that the presence of a fouling layer will alter the nanoscale interactions of the membrane surface with potential compromise of the separation process.

Previous adhesion force measurement studies were performed by Bowen and Doneva [38] on a virgin RO membrane using silica colloid probes with a maximum loading force of 120 nN–140 nN, where force measurements were performed in 10^{-1} M and at pH 9. The force measurements performed on peaks of the membrane revealed an adhesion of 2.3 ± 0.48 mN/m and those performed within the membrane valleys, the adhesion was 8.7 ± 4.0 mN/m. The results obtained at 0.6 M NaCl at pH 9 in the present study revealed adhesion force values of 0.98 nN, which when normalized for colloid radius of 3 μm the adhesion value is 0.33 mN/m, where the differences between the adhesion forces measured by the studies could be due to the very high loading force used by Bowen and Doneva [38]. The colloid would have indented the sample to a greater extent than the present study, hence more surface area contact would have occurred between the sample and the colloid. In addition, the measurements in the present study were at random positions across the membrane surface, with no separation of measurements from peaks and valleys.

4.4. Work of adhesion

The measurement of adhesion from the retraction force curve minima does not account for the mechanisms involved in adhesion (Fig. 1). It is the shape of the force curve adhesion component, which can be described by the work of adhesion, that provides information on interaction mechanisms such as ligand-receptor peeling. The work of adhesion is the work which must be done to separate two adjacent

phases, liquid-liquid or liquid-solid phase as in the case here. The mean work of adhesion values were determined from force measurements at virgin and fouled membranes in 0.6 M NaCl at pH 3, 7 and 9, where the data is shown in Table 2. The distribution of work of adhesion values from the virgin and fouled membranes were summarized using boxplots shown in Fig. 5, where the distribution of all variables were non-parametric. The average values of work of adhesion from the virgin membrane revealed a high adhesion energy at pH 3 (153.6 nJ), which decreased in magnitude at pH 7 (22.8 nJ) and then again at pH 9 (9.9 nJ). The mean work of adhesion values were significantly different ($p < 0.017$) between all pH values. The differences in work of adhesion values could be due to the charge held by the membrane surface in various electrolytic environments (see Section 4.5). The average values of work of adhesion for the fouled membrane showed very little variation between the different pH values, for example at pH 3 the work of adhesion was 16.2 nJ. The mean values were not significantly different ($p < 0.017$), so it was concluded that pH did not have a measurable influence on the values of work of adhesion obtained from the fouled membrane.

The comparison between the values of work of adhesion achieved from the virgin and fouled membrane at each pH value showed that the values of work of adhesion of the virgin membrane at pH 3 and 7 were significantly different and greater in magnitude from that for the fouled membrane ($p < 0.017$). The work of adhesion values at pH 9 were not significantly different ($p > 0.017$).

The work of adhesion and the adhesive force determined from a force measurement are closely linked. However, the adhesive force gives no indication as to how the AFM probe attaches and detaches from a surface. This can be dramatically different when the minimum force recorded in force curves, the adhesive force, is the same. If deformation occurs when the AFM probe interacts with the surface, during the approach and retraction phases of the force measurement, then the work of adhesion will be greater. In addition, another contribution to an increase in the work of adhesion could be an increase in the recruitment of ligands to the interactions, so that the probe has to peel away from the surface and break more bonds. In the present study the high work of adhesion measured at the virgin membrane at pH 3 could be due to the deformation of the surface and/or the increased number of bonds involved in the interaction. This argument demonstrates the potential that AFM force measurement offers the membrane technologist to unravel the processes operating during the formation of fouling layers. In the past this has been restricted by using only AFM adhesive force measurements.

4.5. Streaming potential

The results of zeta potential versus pH for the virgin and process fouled RO membrane at 0.1 M NaCl concentrations are shown in Fig. 6.

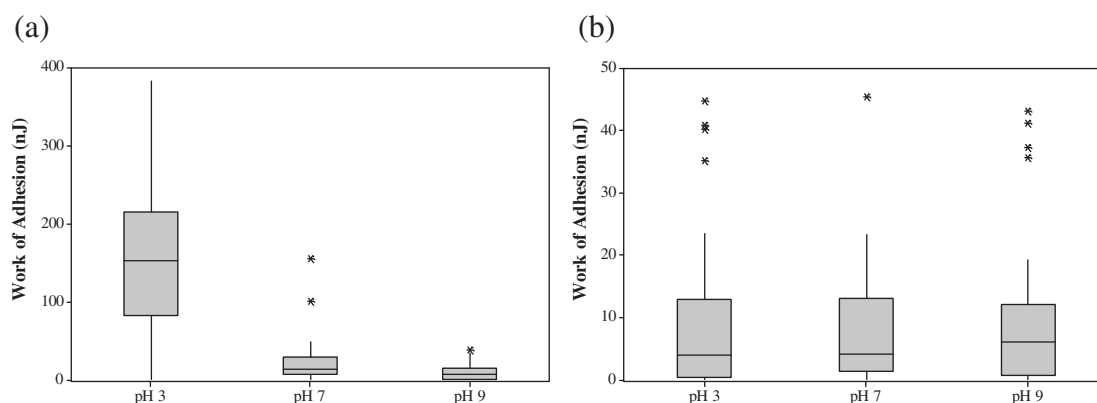


Fig. 5. Variation of work of adhesion for (a) virgin and (b) fouled membranes between different pH values shown in boxplot forms.

The streaming potential equipment was only designed to be operated at low salt concentrations therefore a maximum salt concentration of 0.1 M was used to provide an indication of the surface charge of the membrane. The virgin membrane was positively charged or had no charge at low pH (pH 4, 0 ± 2 mV) and negatively charged at high pH (pH 9, -5.8 ± 3.5 mV), where the IEP was determined to be pH 4.0 for 0.1 M NaCl. The fouled membrane was entirely negatively charged over the pH range, where at pH 3 the zeta potential was -2.3 ± 1.7 mV and at pH 9 was -11.3 ± 3.5 mV and therefore no IEP could be determined.

This differences in AFM force measurements obtained using AFM as a function of pH could be attributed to the change in the ionization state of the membrane surface. The present study measured greatest adhesion and work of adhesion at pH 3, 6.0 nN and 153.6 nJ respectively at 0.6 M NaCl, however there is a suggested agreement with the streaming potential study that indicated that a positive or neutral charge was measured at lower pH. Thus, at pH 3 the membrane would be exhibiting a charge that would not tend to repel the AFM colloid probe and so adhesion parameters would be at their highest. At low pH, the surface charge of the membrane may be positively charged at 0.6 M NaCl and close to the IEP of the membrane where the electric double layer is relatively thin, as shown in Fig. 6 for the virgin membrane at 0.1 M NaCl [42]. As the pH is increased, the membrane may become negatively charged, where the silica colloid is also negatively charged at high pH values [42,43] so as the colloid approaches the membrane surface in these conditions, the colloid could experience increasing electrostatic double-layer repulsive force which opposes the motion of the colloid. Due to the repulsive force, the particle may be prevented from coming into intimate contact with the membrane surface, which leads to a lower adhesion force and work of adhesion.

For the fouled membrane, the adhesion force and work of adhesion values revealed no significant differences as a function of pH. The reason could be the surface charge of the membrane being negative over all pH

values (Fig. 6) which means that the colloid experiences a repulsive force over all pH values which could explain why there was no significant difference of adhesion force and work of adhesion between pH values [44].

Previous research by Al-Amoudi et al. [45] investigated the zeta potential of three virgin and one fouled NF membrane at different pH values and the results agree with our current findings for RO membranes, as the study concluded that the fouled DK (GE Osmonics) membrane were almost negatively charged with no IEP over a range of pH values when compared to a virgin DK membrane.

5. Conclusions

Mechanical measurements obtained from AFM force-distance measurements can provide an assessment of the fouling potential of the membranes by the elucidation of mechanical factors that affect membrane fouling, which has the potential to reduce commissioning studies and optimise process operation. In this study a novel and comprehensive AFM characterisation of the mechanical properties of virgin and industrially fouled membranes was achieved, which detected differences between the virgin and fouled membranes in different electrolyte conditions. The results of the paper suggest that pH control could be investigated to strengthen membranes against chemical and physical challenges, where the increased Young's modulus measured at pH 3 of the virgin membrane indicate, for example, that cleaning at a low pH may be advantageous for the protection of the membrane. A careful balance could be considered by the membrane technologist, which during a cleaning process uses an electrolytic environment that renders the membrane at its strongest, while the biofouling layer could be at its weakest, with the caveat that disruption of the chemical properties of the membrane material are kept to a minimum.

Recent studies have indicated that the mechanical properties of nano-scale polymeric substrata can strongly influence the adhesion of bacteria in aqueous suspensions [30]. However, there are limited examples within the literature on the use of nano-indentation and measurement of the mechanical properties of commercially available membranes and biofilm. Therefore, the mechanical measurements at virgin and biofouled membranes of the present study are extremely timely and such AFM characterisation is a novel technique, when applied to RO membranes, which holds promise for further elucidation of the mechanisms involved in membrane fouling. The present study on industrially fouled membranes has shown that the analysis of AFM force-distance data can be extended beyond simple adhesion measurements to aid diagnosis of processes problems such as fouling, as part of industrial membrane autopsies. It is hoped that this encompassing research study within an industrial context will aid in developing a rational strategy for the prevention of biofouling and biofilm formation, with economic and effective cleaning within

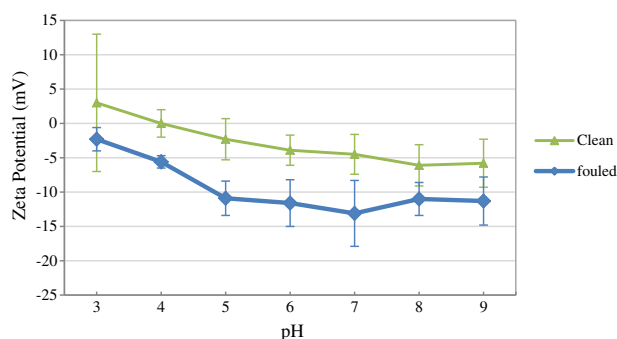


Fig. 6. Zeta potential measurements of virgin and fouled RO membrane at 0.1 M NaCl.

desalination processes, which will maintain efficient membrane operation and prolong membrane life.

Acknowledgments

The authors would like to thank Youngpil Chun and In Seop Chang of the Department of Environmental Science and Engineering, Gwangju Institute of Science and Technology (GIST), Gwangju, South Korea for the supply of fouled membranes. The authors would like to acknowledge the British Council for Research Co-operation Funding and the funding to start this project. Finally we thank Dr. Bob Lovitt of Swansea University for his discussion.

References

- [1] J. Landaburu-Aguirre, R. García-Pacheco, S. Molina, L. Rodríguez-Sáez, J. Rabadán, E. García-Calvo, Fouling prevention, preparing for re-use and membrane recycling. Towards circular economy in RO desalination, *Desalination* 393 (2016) 16–30.
- [2] Y. Wyart, G. Georges, C. Deumie, C. Amra, P. Moulin, Membrane characterization by microscope methods: multiscale structure, *J. Membr. Sci.* 315 (2008) 82–92.
- [3] Y. Chun, P.T. Ha, L. Powell, J. Lee, D. Kim, D. Choi, R.W. Lovitt, I.S. Kim, S.S. Mitra, I.S. Chang, Exploring microbial communities and differences of cartridge filters (CFs) and reverse osmosis (RO) membranes for seawater desalination processes, *Desalination* 298 (2012) 85–92.
- [4] V.M. Kochkodan, N. Hilal, V.V. Goncharuk, L. Al-Khatib, T.I. Levadna, Effect of the surface modification of polymer membranes on their microbiological fouling, *Colloid J.* 68 (3) (2006) 267–273.
- [5] J. Zhang, K. Northcott, M. Duke, P. Scales, S.R. Gray, Influence of pre-treatment combinations on RO membrane fouling, *Desalination* 393 (2016) 120–126.
- [6] M.N. Abu Seman, M. Khayet, Z.I. Bin Ali, N. Hilal, Reduction of nanofiltration membrane fouling by UV-initiated graft polymerization technique, *J. Membr. Sci.* 355 (1–2) (2010) 133–141.
- [7] M. Khayet, M.N.A. Seman, N. Hilal, Response surface modeling and optimization of composite nanofiltration modified membranes, *J. Membr. Sci.* 349 (1–2) (2010) 113–122.
- [8] W.R. Bowen, N. Hilal, R.W. Lovitt, P.M. Williams, Atomic force microscope studies of membranes: surface pore structures of Diaflo ultrafiltration membranes, *J. Colloid Interface Sci.* 180 (2) (1996) 350–359.
- [9] W.R. Bowen, N. Hilal, R.W. Lovitt, A.O. Sharif, P.M. Williams, Atomic force microscope studies of membranes: force measurement and imaging in electrolyte solutions, *J. Membr. Sci.* 126 (1) (1997) 77–89.
- [10] N. Hilal, H. Al-Zoubi, N.A. Darwish, A.W. Mohammad, M. Abu Arabi, A comprehensive review of nanofiltration membranes: treatment, pretreatment, modelling, and atomic force microscopy, *Desalination* 170 (3) (2004) 281–308.
- [11] C.J. Wright, I. Armstrong, The application of atomic force microscopy force measurements to the characterization of microbial surfaces, *Surf. Interface Anal.* 38 (2006) 1419–1428.
- [12] I.J. Roh, J.-J. Kim, S.Y. Park, Mechanical properties and reverse osmosis performance of interfacially polymerized polyamide thin films, *J. Membr. Sci.* 197 (2002) 199–210.
- [13] P.J. Evans, M.R. Bird, D. Rogers, C.J. Wright, Measurement of polyphenol-membrane interaction forces during the ultrafiltration of black tea liquor, *Colloids Surf. A Physicochem. Eng. Asp.* 335 (1–3) (2009) 148–153.
- [14] J.-Y. Tian, Z.-L. Chen, Y.-L. Yang, H. Liang, J. Nan, G.-B. Li, Consecutive chemical cleaning of fouled PVC membrane using NaOH and ethanol during ultrafiltration of river water, *Water Res.* 44 (1) (2010) 59–68.
- [15] H. Ivnitsky, I. Katz, D. Minz, G. Volvovic, E. Shimoni, E. Kesselman, R. Semiat, C.G. Dosoretz, Bacterial community composition and structure of biofilms developing on nanofiltration membranes applied to wastewater treatment, *Water Res.* 41 (17) (2007) 3924–3935.
- [16] D.J. Johnson, N.J. Miles, N. Hilal, Quantification of particle-bubble interactions using atomic force microscopy: a review, *Adv. Colloid Interf. Sci.* 127 (2) (2006) 67–81.
- [17] W.R. Bowen, N. Hilal, R.W. Lovitt, C.J. Wright, A new technique for membrane characterisation: direct measurement of force of adhesion of a single particle using an atomic force microscope, *J. Membr. Sci.* 139 (1998) 269–274.
- [18] W.R. Bowen, N. Hilal, R.W. Lovitt, C.J. Wright, Characterisation of membrane surfaces: direct measurement of biological adhesion using an atomic force microscope, *J. Membr. Sci.* 154 (1999) 205–212.
- [19] L. Zhang, Q.-Q. Ni, T. Natsuki, Mechanical properties of polybenzimidazole reinforced by carbon nanofibers, *Adv. Mater. Res.* 47–50 (2008) 302–305.
- [20] H. Xu, K. Chen, X. Guo, J. Fang, J. Yin, Synthesis of hyperbranched polybenzimidazoles and their membrane formation, *J. Membr. Sci.* 288 (2007) 255–260.
- [21] E.A. Franceschini, H.R. Corti, Elastic properties of nafion, polybenzimidazole and poly [2,5-benzimidazole] membranes determined by AFM tip nano-indentation, *J. Power Sources* 188 (2009) 379–386.
- [22] A.-Y. Jee, M. Lee, Comparative analysis on the nanoindentation of polymers using atomic force microscopy, *Polym. Test.* 29 (2010) 95–99.
- [23] T.-H. Fang, W.-J. Chang, S.-L. Tsai, Nanomechanical characterisation of polymer using atomic force microscopy and nanoindentation, *Microchem. J.* 36 (2005) 55–59.
- [24] J.Y. Chung, J.-H. Lee, K.L. Beers, C.M. Stafford, Stiffness, strength and ductility of nanoscale thin films and membranes: a combined wrinkling-cracking methodology, *Nano Lett.* 11 (2011) 3361–3365.
- [25] J. Llanos, P.M. Williams, S. Cheng, D. Rogers, C. Wright, A. Perez, P. Canizares, Characterization of a ceramic ultrafiltration membrane in different operational states after its use in a heavy-metal ion removal process, *Water Res.* 44 (2010) 3522–3530.
- [26] L.C. Powell, A. Sowadan, S. Khan, C.J. Wright, K. Hawkins, E. Onsøyen, R. Myrvold, K.E. Hill, D.W. Thomas, The effect of alginate oligosaccharides on the mechanical properties of Gram-negative biofilms, *Biofouling* 29 (4) (2013) 413–421.
- [27] C.J. Wright, M.K. Shah, L.C. Powell, I. Armstrong, Application of AFM from microbial cell to biofilm, *Scanning* 32 (2010) 134–149.
- [28] D.P. Bakker, F.M. Huijs, J. de Vries, J.W. Klijnstra, H.J. Busscher, H.C. van der Mei, Bacterial deposition to fluoridated and non-fluoridated polyurethane coatings with different elastic modulus and surface tension in a parallel plate and a stagnation point flow chamber, *Colloids Surf. B Biointerfaces* 32 (2003) 179–190.
- [29] S. Lee, M. Elimelech, Relating organic fouling of reverse osmosis membranes to intermolecular adhesion forces, *Environ. Sci. Technol.* 40 (2006) 980–987.
- [30] J.A. Lichter, M.T. Thompson, M. Delgadillo, T. Nishikawa, M.F. Rubner, K.J. Van Vliet, Substrate mechanical stiffness can regulate adhesion of viable bacteria, *Biomacromolecules* 9 (2008) 1571–1578.
- [31] Y.J. Oh, N.R. Lee, W. Jo, W.K. Jung, J.S. Lim, Effects of substrates on biofilm formation observed by atomic force microscopy, *Ultramicroscopy* 109 (2009) 874–880.
- [32] W.A. Ducker, T.J. Senden, R.M. Pashley, Direct measurement of colloidal forces using an atomic force microscope, *Nature* 353 (1991) 239–241.
- [33] A. Touhami, B. Nysten, Y.F. Dufrene, Nanoscale mapping of the elasticity of microbial cells by atomic force microscopy, *Langmuir* 19 (2003) 4539–4543.
- [34] S.-Y. Kwak, D.W. Ihm, Use of atomic force microscopy and solid-state NMR spectroscopy to characterise structure-property-performance correlation in high flux reverse osmosis (RO) membranes, *J. Membr. Sci.* 158 (1999) 143–153.
- [35] M. Karime, S. Bougoucha, B. Hamrouni, RO membrane autopsy of Zarzis brackish water desalination plant, *Desalination* 220 (2008) 258–266.
- [36] E.O. Mohamedou, D.B.P. Surarez, F. Vince, P. Jaouen, M. Pontie, New lives for old reverse osmosis (RO) membranes, *Desalination* 53 (2010) 62–70.
- [37] K. Bouso, B. Van der Bruggen, A. Volodin, J. Snauwaert, C. Van Hasendonck, C. Vandecasteele, Roughness and hydrophobicity studies of nanofiltration membranes using different modes of AFM, *J. Colloid Interface Sci.* 286 (2005) 632–638.
- [38] W.R. Bowen, T.A. Doneva, Atomic force microscopy studies of membranes: effect of surface roughness on double-layer interactions and particle adhesion, *J. Colloid Interface Sci.* 229 (2000) 544–549.
- [39] J.E. Elliott, M. Macdonald, J. Nie, C.N. Bowman, Structure and swelling of poly (acrylic acid) hydrogels: effect of pH, ionic strength, and dilution on the crosslinked polymer structure, *Polymer* 45 (2004) 1503–1510.
- [40] J. Yang, S. Lee, E. Lee, J. Lee, S. Hong, Effect of solution chemistry on the surface property of reverse osmosis membranes under seawater conditions, *Desalination* 249 (2009) 148–161.
- [41] A. Hourai, J. Picard, H. Habarou, L. Galas, H. Vaudry, V. Heim, P. Di Martino, Rheology of biofilms formed at the surface of NF membranes in a drinking water production unit, *Biofouling* 24 (4) (2008) 235–240.
- [42] E.M. Vrijenhoek, S. Hong, M. Elimelech, Influence of membrane surface properties on initial rate of colloidal fouling of reverse osmosis and nanofiltration membranes, *J. Membr. Sci.* 188 (2001) 115–128.
- [43] X. Sheng, Y.P. Ting, S.O. Pehkonen, The influence of ionic strength, nutrients and pH on bacterial adhesion to metals, *J. Colloid Interface Sci.* 321 (2008) 256–264.
- [44] D. Elzo, I. Huisman, E. Middlelink, V. Gekas, Charge effects on inorganic membrane performance in a cross-flow microfiltration process, *Colloids Surf. A Physicochem. Eng. Asp.* 138 (1998) 145–159.
- [45] A. Al-Amoudi, P. Williams, S. Mandale, R.W. Lovitt, Cleaning results of new and fouled nanofiltration membrane characterized by zeta potential and permeability, *Sep. Purif. Technol.* 54 (2007) 234–240.